Chemical Engineering Journal 399 (2020) 125755

Contents lists available at ScienceDirect

Chemical Engineering Journal

journal homepage: www.elsevier.com/locate/cej

Superhydrophobic n-octadecylsiloxane (PODS)-functionalized PDA-PEI film as efficient water-resistant sensor for ppb-level hexanal detection

Luyu Wang[a,*], Yunling Wu[b], Gaojie Li[c], Hui Xu[d], Junkuo Gao[a,*], Qichun Zhang[e,*]

[a] Institute of Functional Porous Materials, The Key Laboratory of Advanced Textile Materials and Manufacturing Technology of Ministry of Education, School of Materials Science and Engineering, Zhejiang Sci-Tech University, Hangzhou 310018, China
[b] Institute of Functional Nano & Soft Materials (FUNSOM), Jiangsu Key Laboratory for Carbon-Based Functional Materials and Devices, Soochow University, Suzhou 215123, China
[c] School of Physics and Engineering, Henan University of Science and Technology, Luoyang 471023, China
[d] College of Materials Science and Engineering, China Jiliang University, Hangzhou 310018, China
[e] School of Materials Science & Engineering, Nanyang Technological University, Singapore 639798, Singapore

HIGHLIGHTS

- Detection of ppb level hexanal was first realized based on QCM.
- The sensor detected hexanal vapor stably in high humidity environment.
- The false alarm of humidity can be ignored.
- The core sensing site was found out by simulation calculation.

GRAPHICAL ABSTRACT

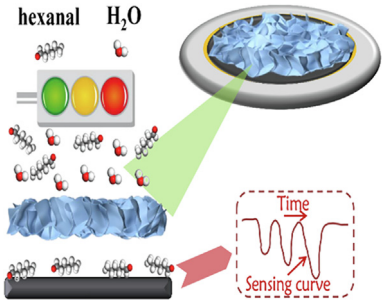

ARTICLE INFO

Keywords:
Quartz crystal microbalances
Water-resistant
Polymer
Hexanal
Gas sensor

ABSTRACT

The detection of hexanal vapor in ppb (part per billion) concentration is an unresolved and indispensable issue. Here we report a polydopamine-polyethyleneimine (PDA-PEI) copolymer film with rich imino groups to sense 50 ppb hexanal vapor through the formation of the reversible hydrogen bonds with hexanal. We found that the water-resistance could be further improved by attaching superhydrophobic n-octadecylsiloxane (PODS) onto the surface of PDA-PEI film. The chemical adsorption mode and the core role of imino group for the hexanal detection have been validated by combining experiment methods with theory calculations. A quartz crystal microbalance (QCM) platform modified with this film was employed as a hexanal vapor sensor under ambient conditions, which possessed several advantages including the high response of 34.8 Hz to 250 ppb hexanal, low detection limit of 50 ppb hexanal at 25 °C, and good water-resistance.

1. Introduction

Among various volatile organic compounds (VOCs), organic aldehydes are one of volatile gases from human metabolites or by-products generated by vegetation [1,2]. Meanwhile, as significant raw chemicals, organic aldehydes have also been widely used in a variety of areas such as the timber textile products, food additives, catalysis industry, etc. [3,4]. Organic aldehydes can evaporate into air from construction materials, inferior textiles, wastewater, factory emissions, human sweat, etc. [5]. The excess gaseous organic aldehydes in the air would

* Corresponding authors.
E-mail addresses: wangluyu@zstu.edu.cn (L. Wang), jkgao@zstu.edu.cn (J. Gao), qczhang@ntu.edu.sg (Q. Zhang).

https://doi.org/10.1016/j.cej.2020.125755
Received 25 March 2020; Received in revised form 27 May 2020; Accepted 1 June 2020
Available online 04 June 2020
1385-8947/

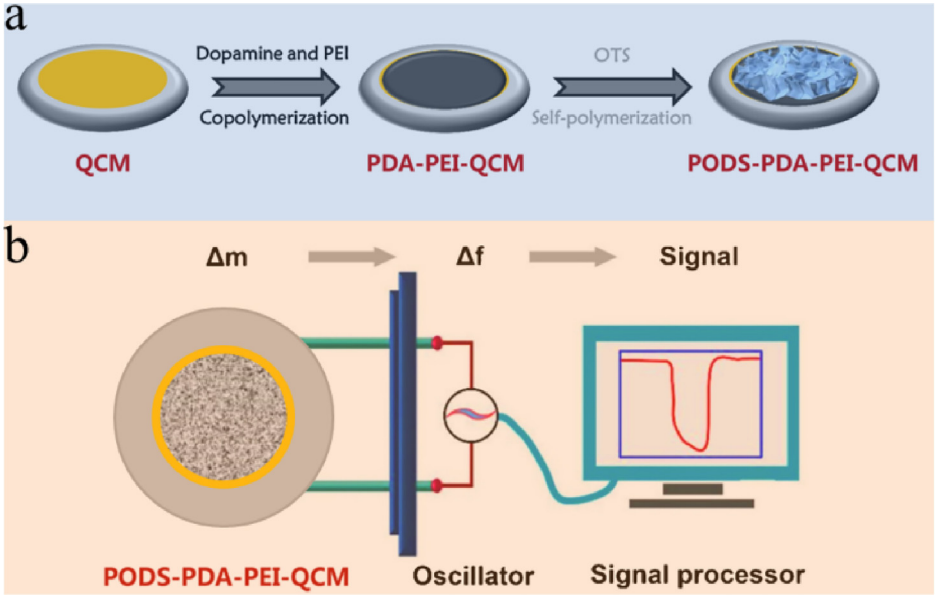

Fig. 1. (a) Scheme of preparation of PODS covered PDA-PEI-QCM. (b) QCM schematic view.

Table 1
The comparison of hexanal sensing properties between the reported sensing materials and PODS-PDA-PEI in this work.

Reference	Material	Limit of detection	Response time	Recovery time
[23]	1,2-distearoyl-*sn*-glycero-3-phosphoethanolamine-N-[methoxy (polyethylene glycol)2000]	140 ppm	> 200 s	> 180 s
[24]	hydrophobic molecularly imprinted polymers (MIPs)	2 ppm	45 s	> 200 s
[25]	Span 80	10 ppm	–	–
[26]	hexanoic acid template based polyacrylic acid-MIP	5ul/100 ml	–	–
[27]	hydrophobic Cu(I)-Cys composite	5 ppm	–	–
This work	PODS-PDA-PEI	50 ppb	24 s	23 s

heavily damage human health (even causing cancer), so it is imperative to detect gaseous organic aldehydes in trace level [6,7]. Sensors are ideal devices for detecting toxic and harmful substances, because they have the advantages of portability, low cost, easy-design, and quick detection [8–16]. For detecting organic aldehydes, especially formaldehyde and acetaldehyde, scientists have developed a considerable number of gas sensors [17,18]. Hexanal is also a common and neglected organic aldehyde, and its vapor is usually released from wood products and fruit peel oil. When its concentration is higher than 2 ppm (part per million), hexanal vapor stimulates the eyes, nose and other parts of human body, and even aggravates the inflammation [19]. In addition, the concentration of gaseous hexanal in exhaled breath can reflect the human health. For example, the concentration of hexanal in exhaled breath of lung cancer patients is ppb (part per billion) level. As a contrast, the exhaled breath of healthy people is almost free of hexanal [20,21]. Therefore, in order to facilely detect the lung cancer as early as possible and prevent its deterioration, it is necessary to develop selective gas sensors capable of detecting hexanal vapor in ppb concentration.

Quartz crystal microbalance (QCM) is a small-size mass-sensitive device. The most obvious advantages of QCM over other sensors are high sensitivity, low cost, and working at room temperature [22–27]. The surficial quality of QCM can be changed by adsorbing gas, resulting in a change in its frequency [28,29]. The quality change and the frequency change are converted by Sauerbrey equation [30]. Based on the above theories, scientists constructed the QCM sensors toward specific gases by modifying various sensing materials. The special force between sensing material and gas is the basis to ensure the sensitivity and selectivity of QCM sensor [31]. Among the developed QCM sensing materials, organic polymers are the most important ones [32,33]. Compared with inorganic materials, organic polymers have a wide variety of functional groups, which can be adjusted by post-synthesis method to meet the detection needs of different gases [34]. The detection of ammonia, toluene, formaldehyde and other gases has been achieved by using various functionalized polymers [35–37]. For detecting hexanal vapor, a QCM sensor based on hexanal-molecularly-imprinted polymer is capable of detecting hexanal vapor in the concentration range of 1 ppm to 100 ppm [24]. However, currently no sensor capable of detecting ppb hexanal vapor is reported.

As a bio-inspired organic polymer, polydopamine (PDA) acts as QCM sensing material to detect formaldehyde gas with ppb concentration. The imino group of PDA plays the key role in the sensing process and has shown good sensing performance to aldehyde group in formaldehyde molecule at room temperature. The sensing mechanism is based on hydrogen bonding adsorption [38]. To target ppb level sensitivity to hexanal vapor containing aldehyde group, it is necessary for sensing material to possess more imino groups to largely adsorb hexanal through hydrogen bonds. Polydopamine-polyethyleneimine (PDA-PEI) copolymer can be facilely synthesized by adding polyethyleneimine (PEI) in the self-polymerization process of PDA. This copolymer has more imino groups than PDA [39]. Inspired by these theories, we hypothesized that imino-rich PDA-PEI copolymer might have strong adsorptive sensing ability to hexanal vapor.

Herein, we synthesized PDA-PEI film on the surface of QCM and examined the sensing performance of hexanal vapor. We found that these sensors could detect ppb level of hexanal vapor effectively. Afterwards, a water-resistant hexanal sensor was obtained by covering a layer of superhydrophobic n-octadecylsiloxane (PODS) on the surface of PEI-PDA film to protect the sensing material from environmental humidity [40], as shown in Fig. 1 and experimental section. In different high humidity environments, this sensor showed excellent stability in hexanal vapor detection. The sensitivity of this sensor is also prominent,

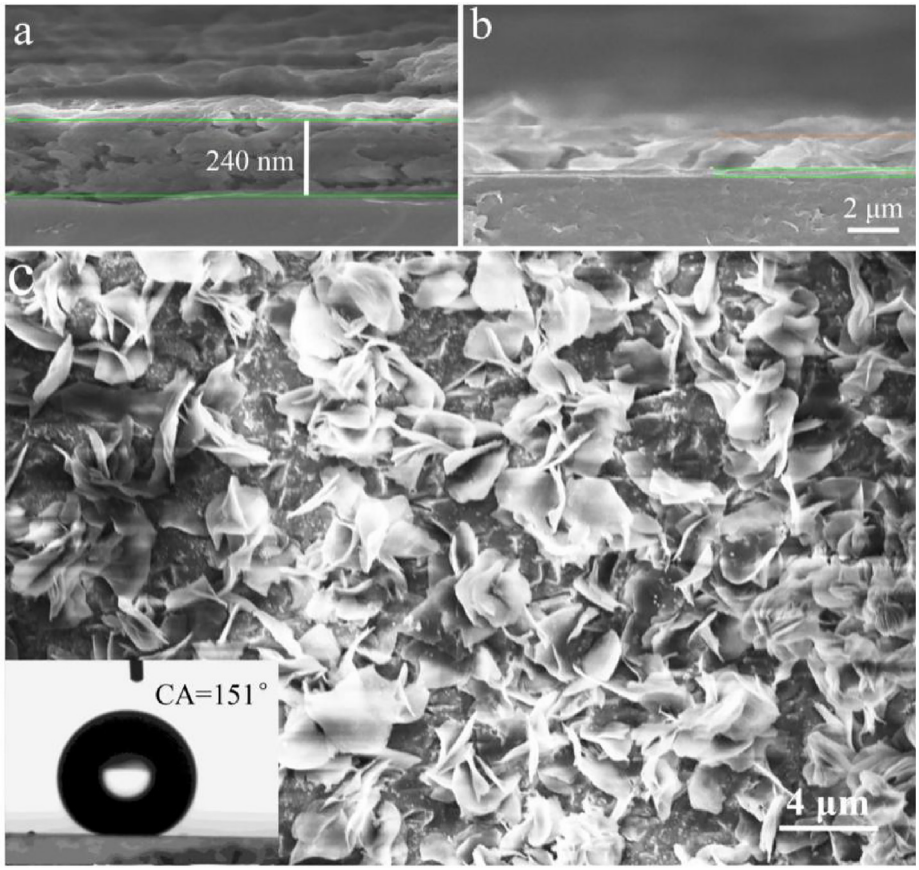

Fig. 2. (a) Cross-section SEM image of the PDA-PEI-QCM. (b) Cross-section SEM image of the PODS-PDA-PEI-QCM. (c) Top view SEM image of the PODS-PDA-PEI-QCM, and the insert show its contact angle test result.

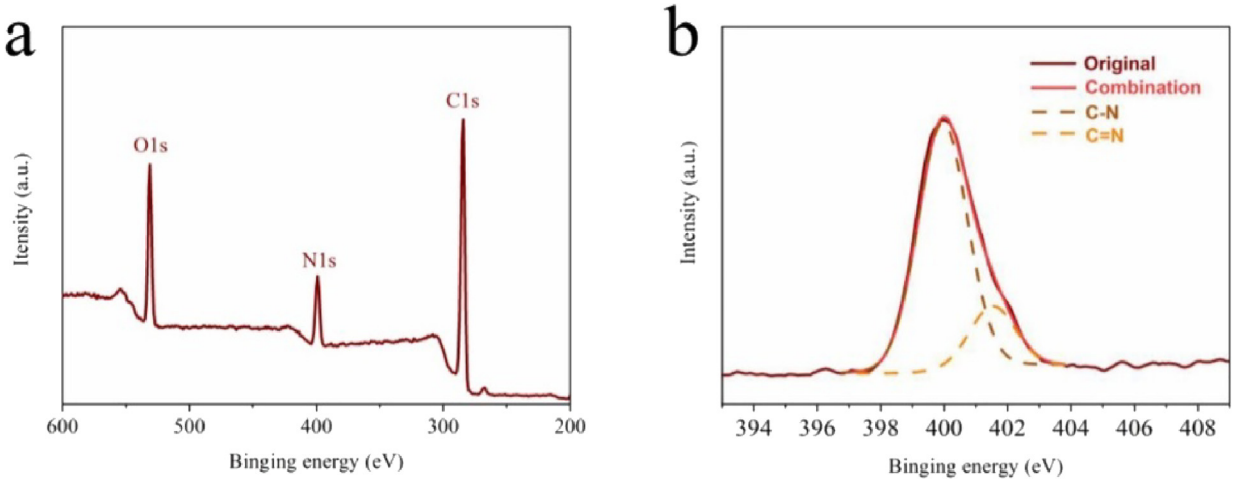

Fig. 3. (a) The survey scan and (b) N 1s XPS spectrum of PDA-PEI.

and its response to 50 ppb hexanal reaches 6 Hz, demonstrating that it is the best water-resistant hexanal sensor reported to date because of this important sensitivity (ppb level). Table 1 lists the hexanal sensing parameters of the reported hexanal sensing materials and PODS-PDA-PEI based on QCM, including limit of detection, response time, and recovery time. The response time (recovery time) was defined as the time taken by the sensor to achieve 90% of the total response (recovery) change. Compared with the previously reported sensing materials, the material we designed has lower detection limit, shorter response time, and shorter recovery time. Due to its excellent performance, the hexanal sensor is expected to be used to detect additional additives in wood products and fruit additives, as well as diagnose lung cancer by detect exhalation in the future.

2. Experimental section

Tris (hydroxymethyl) aminomethane hydrochloride (Tris, 99%), dopamine hydrochloride (98%) and polyethylene-imine (PEI, Mw = 600 Da) were purchased from Aladdin, octadecyltrichlorosilane (OTS) was purchased from Acros Organics, and other chemical reagents were from Gaojing Chemical Plant.

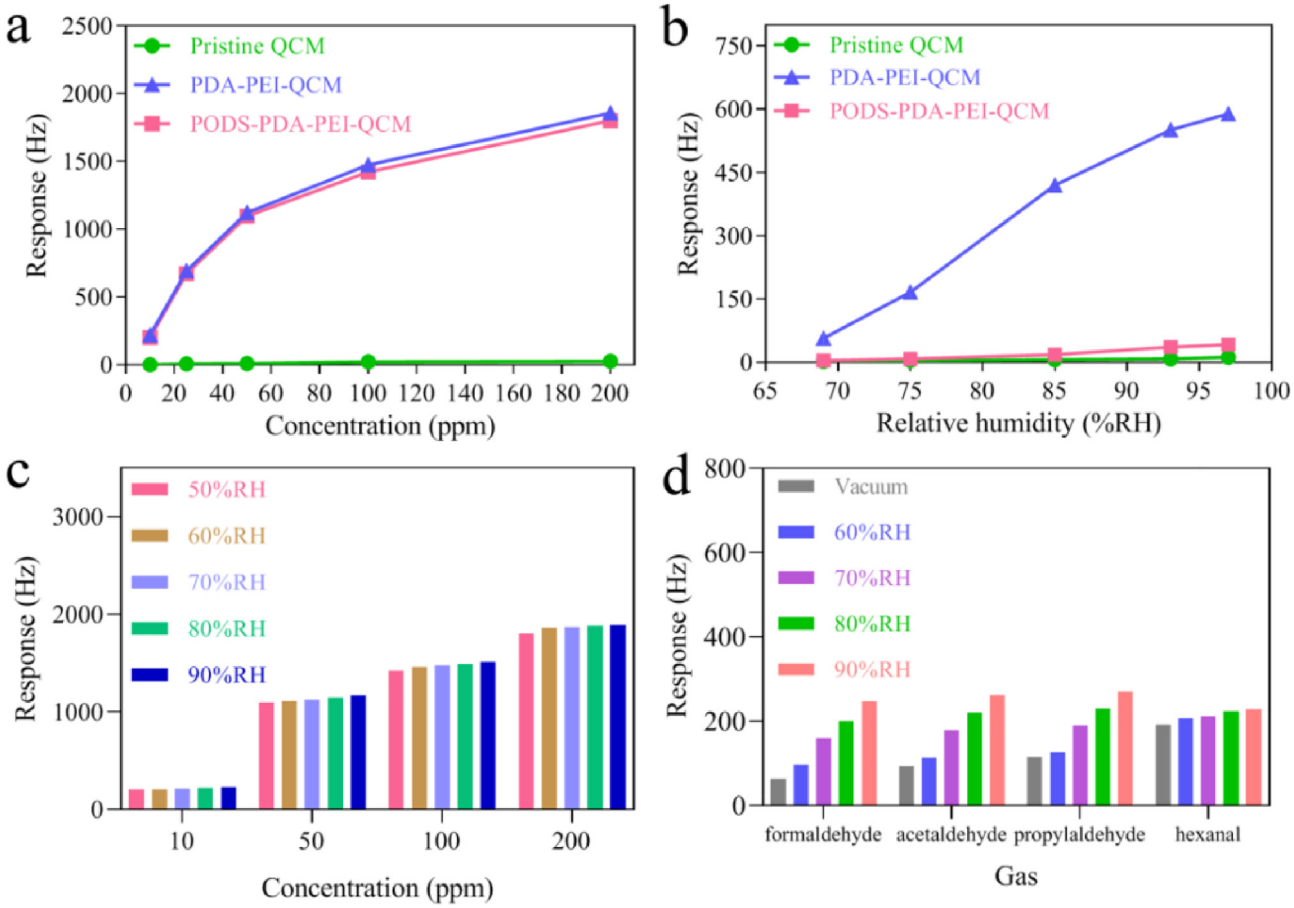

Fig. 4. (a) The relationship between the responses of the sensors and the hexanal concentrations. (b) The relationships between the responses of the sensors and the corresponding relative humidity. (c) Response of PODS-PDA-PEI-QCM sensor exposed to 10, 50, 100, and 200 ppm of hexanal at some relative humidity environments. (d) Response of PODS-PDA-PEI-QCM sensor exposed to four kinds of organic aldehydes (10 ppm) at some relative humidity environments.

Table 2
The summary of sensing materials for detecting 50 ppb hexanal based on QCM.

Material	Response	Response time	Recovery time	Lifetime	Sensitivity value
PDA-PEI-QCM	6.1 Hz	22 s	24 s	< 2 weeks	0.122 Hz/ppb
PODS-QCM	0	–	–	–	–
PODS-PDA-PEI- QCM	5.9 Hz	24 s	23 s	> 4 weeks	0.118 Hz/ppb

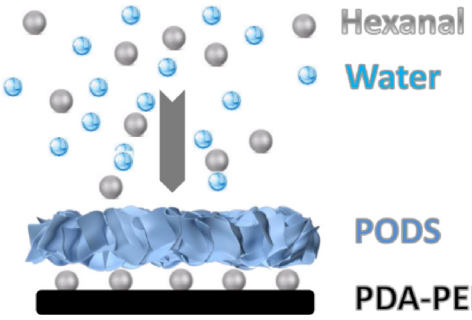

Fig. 5. Superhydrophobic PODS prevents water clusters from contacting PDA-PEI film.

2.1. Preparing PODS covered PDA-PEI film on QCM

QCM was cleaned with acetone and DI water. PDA-PEI copolymer and PODS was synthesized according to the previous reports [39–41]. First, PEI (1.8 mg ml^{-1}) and dopamine hydrochloride (1.8 mg ml^{-1}) were dissolved into a Tris buffer solution (pH = 8.5) with a molar concentration of 50 mmol/L. Then, the cleaned QCM was immersed in the above solution under shaking for uniform deposition at 298 K for 4 h. After that, uniform PDA-PEI thin film was adhered on the surface of QCM. The coated QCM was washed with DI water and dried in a vacuum drying oven at 313 K for 20 h. The QCM coated with PDA-PEI film was named as PDA-PEI-QCM. Subsequently, we took the PDA-PEI-QCM out of the oven and dropped OTS on its surface. Then, the QCM was spun at high speed (typically with 4000 rpm) to create a uniform coating. The coating QCM was immersed in acetone for 5 s, and then taken out, dried in the air for 60 s, and cured in a vacuum drying oven at 363 K for 0.5 day. The PODS-deposited PDA-PEI-QCM was named as PODS-PDA-PDA-QCM. Finally, PODS-PDA-PEI on the surface of QCM (except electrode) was erased by medical cotton swabs infiltrated with alcohol.

2.2. Characterization, gas sensing performance test, and simulation calculations

The characterization methods of the as-synthesized materials are

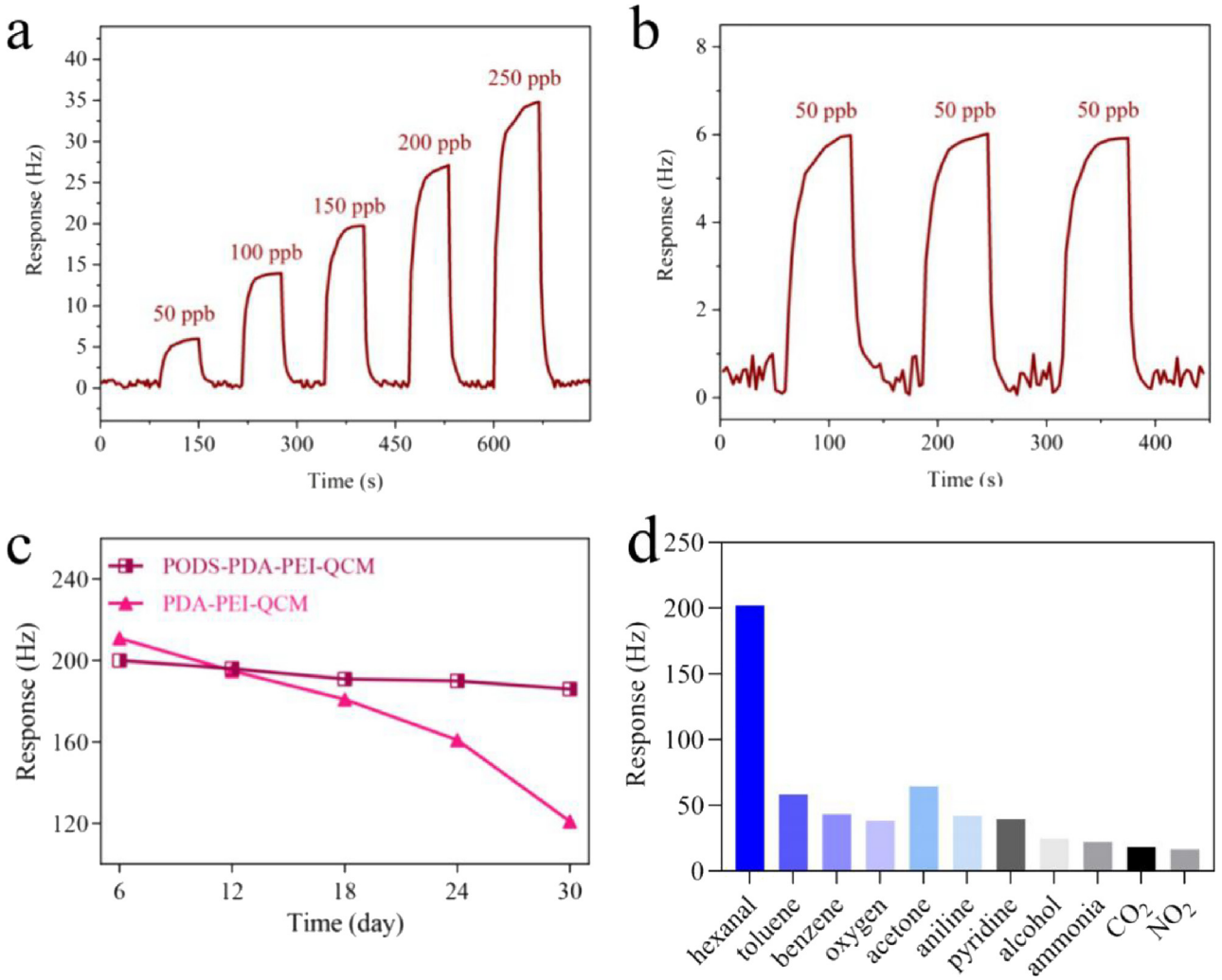

Fig. 6. (a) Response of PODS-PDA-PEI-QCM to various hexanal concentrations. (b) Reproducibility of PODS-PDA-PEI-QCM for successive detection of 50 ppb hexanal. (c) Long-term stability of PODS-PDA-PEI-QCM and PDA-PEI-QCM to 10 ppm hexanal. (d) Selectivity of 10 ppm for various gases.

shown in the Supporting information (Note S1). The test process of the QCM-based gas sensor is described in the Supporting information (Note S2, Note S3, Fig. S1, and Fig. S2). The method and parameters of Gaussian simulation can be found in the Supporting information (Note S4).

3. Result and discussion

3.1. Morphology and structural characterization

PODS can self-polymerize on all surfaces facilely and quickly to enhance hydrophobicity without destroying the surficial structures [41]. The synthetic process of materials and the fabrication process of sensors are illustrated in Fig. 1 (more details in the Experimental Section). Fig. 2 shows the SEM images of the PDA-PEI-QCM and PODS-PDA-PEI-QCM. The PDA-PEI film in Fig. 2a is relatively dense and uniform with a thickness of approximately 240 nm. According to the literature, the crosslinking reaction between PEI and PDA occurs in Tris solution to form Schiff base [42]. As shown in Fig. S3, the infrared spectrum of the PDA-PEI film illustrates that this copolymer film contains C=N bonds (a new absorption band at 1663 cm^{-1}), which do not exist in PDA, confirming the formation of Schiff base and the occurrence of the crosslinking reaction [39]. The result of XPS test in Fig. 3a also shows that the PDA-PEI film consists of three elements: C, N, and O. As shown in Fig. 3b, the N 1s spectra of PDA-PEI film displays the C=N component, which is consistent with the results of infrared spectrum [42]. In addition, as shown in Fig. S4, the UV–vis spectrum of PDA-PEI exhibits an absorption peak around 367 nm, which was associated with the formation of C=C–C=N and C=C–C=O. Meanwhile, the absorption peak around 410 nm of PDA disappears. These characterizations demonstrate the successful synthesis of PDA-PEI [39]. As shown in Fig. 2b, the PODS layer is much thicker than PDA-PEI layer, reaching about 7 μm. The infrared spectrum (Fig. S5) and XRD pattern (Fig. S6) of PODS demonstrate the successful synthesis. Besides, Fig. 2c shows that the as-synthesized PODS is petal-like and has some gaps that can expose part of the underlying PDA-PEI. The related characterizations for three compared materials (PDA-PEI, PODS, and PODS-PDA-PEI) are listed in Supporting Information, including TEM (Fig. S7), XRD (Fig. S8), FT-IR (Fig. S9), and XPS (Fig. S10). TEM images show that the PDA-PEI is particle-like, and PODS is sheet-like. PODS-PDA-PEI contains the above two substances. The XRD spectrum of PODS-PDA-PEI contains two corresponding peaks of PDA-PEI and PODS. The FT-IR spectrum of PODS-PDA-PEI has many characteristic peaks. These characteristic peaks can be found dividedly in PDA-PEI and PODS at the same position. The XPS survery spectrum of PODS-PDA-PEI contains four elements of O, N, C, and Si. N element is derived from PDA-PEI, and Si element is derived from PODS. The above characterization results prove that there are two substances co-existing in the final PODS-PDA-PEI, including PODS-PDA and PODS. Meanwhile, the water-droplet contact angle of PODS-PDA-PEI-QCM is 151°, which is bigger than

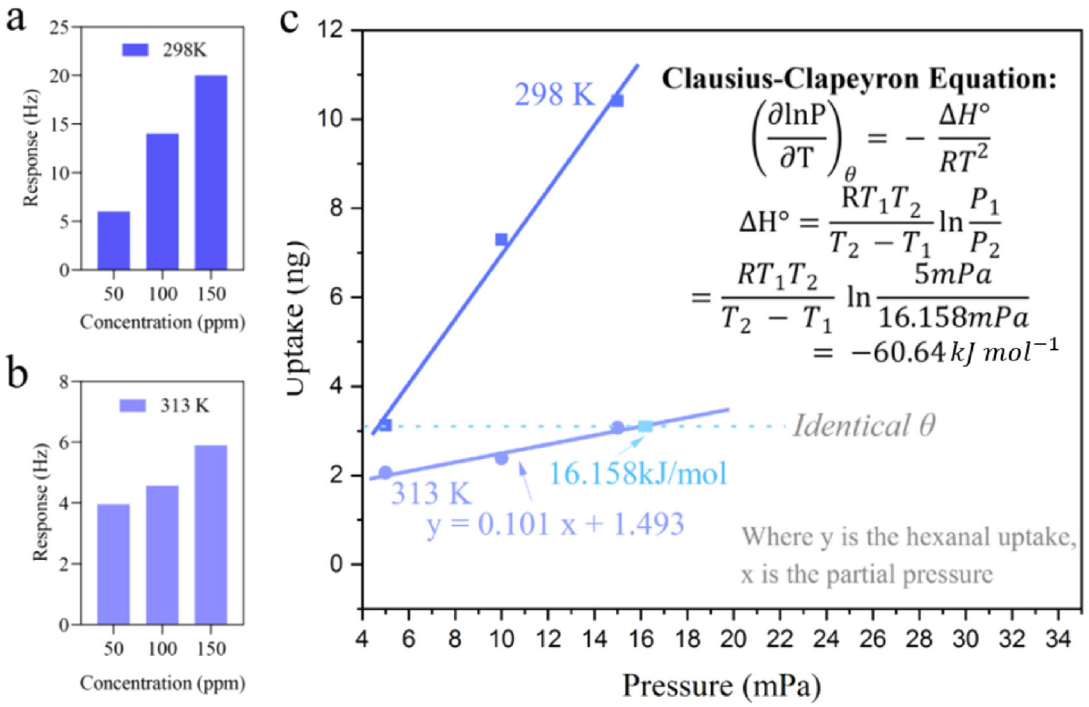

Fig. 7. Responses of PODS-PDA-PEI-QCM at (a) 298 K and (b) 313 K to hexanal with different concentrations of 50, 100, and 150 ppb. Based on temperature-varied micro-gravimetric curves, the plotted isotherms are used to extract the ΔH. (c) Based on the experimental results of (a) and (b), two isotherms are plotted to calculate the value of ΔH.

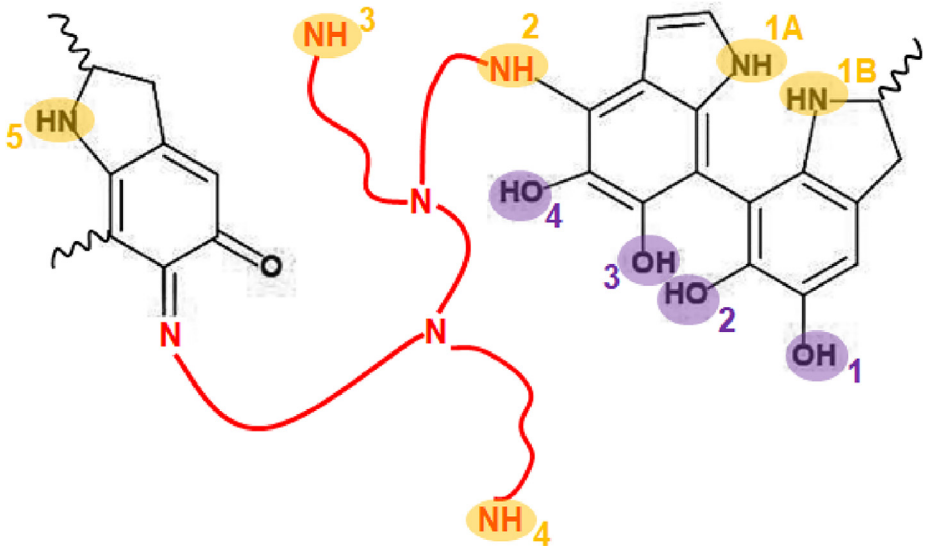

Fig. 8. The structural formula of PDA-PEI monomer.

150°, showing its superhydrophobic property [43].

3.2. Gas sensing studies

Fig. 4a and b exhibit the hexanal-sensing and humidity-sensing performances of these three fabricated sensors, including pristine QCM, PDA-PEI-QCM, and PODS-PDA-PEI-QCM. Within all concentrations of hexanal (10–200 ppm), PDA-PEI-QCM and PODS-PDA-PEI-QCM sensors exhibit higher response in comparison with pristine QCM. The response is positively correlated with hexanal concentration (Fig. 4a). At the same time, the response of PODS-PDA-PEI-QCM is very close to that of PDA-PEI-QCM. Conversely, as shown in Fig. 4b, the responses of PODS-PDA-PEI-QCM to high humidities (69–97% RH) are much smaller than those of PDA-PEI-QCM, indicating the water-resistant role of super-hydrophobic PODS. Compared with PDA-PEI-QCM, PODS-PDA-PEI-QCM has matched response to hexanal vapor, and it is not easy to have false alarm response to high humidity. There is no doubt that PODS-PDA-PEI-QCM is a better sensor for further exploration. Table 2 lists the main sensing parameter data of the three sensors to 50 ppb hexanal, including PDA-PEI-QCM, PODS-QCM, and PODS-PDA-PEI-QCM. The response time is defined as the time taken by the sensor to achieve 90% of the total response, and the recovery time is defined as the time taken by the sensor to achieve 90% of the total recovery change. PODS-QCM has no response to 50 ppb hexanal. Comparing PDA-PEI-QCM and PODS-PDA-PEI-QCM, it is obvious that the introduction of PODS has little negative effect on hexanal sensing performance, including

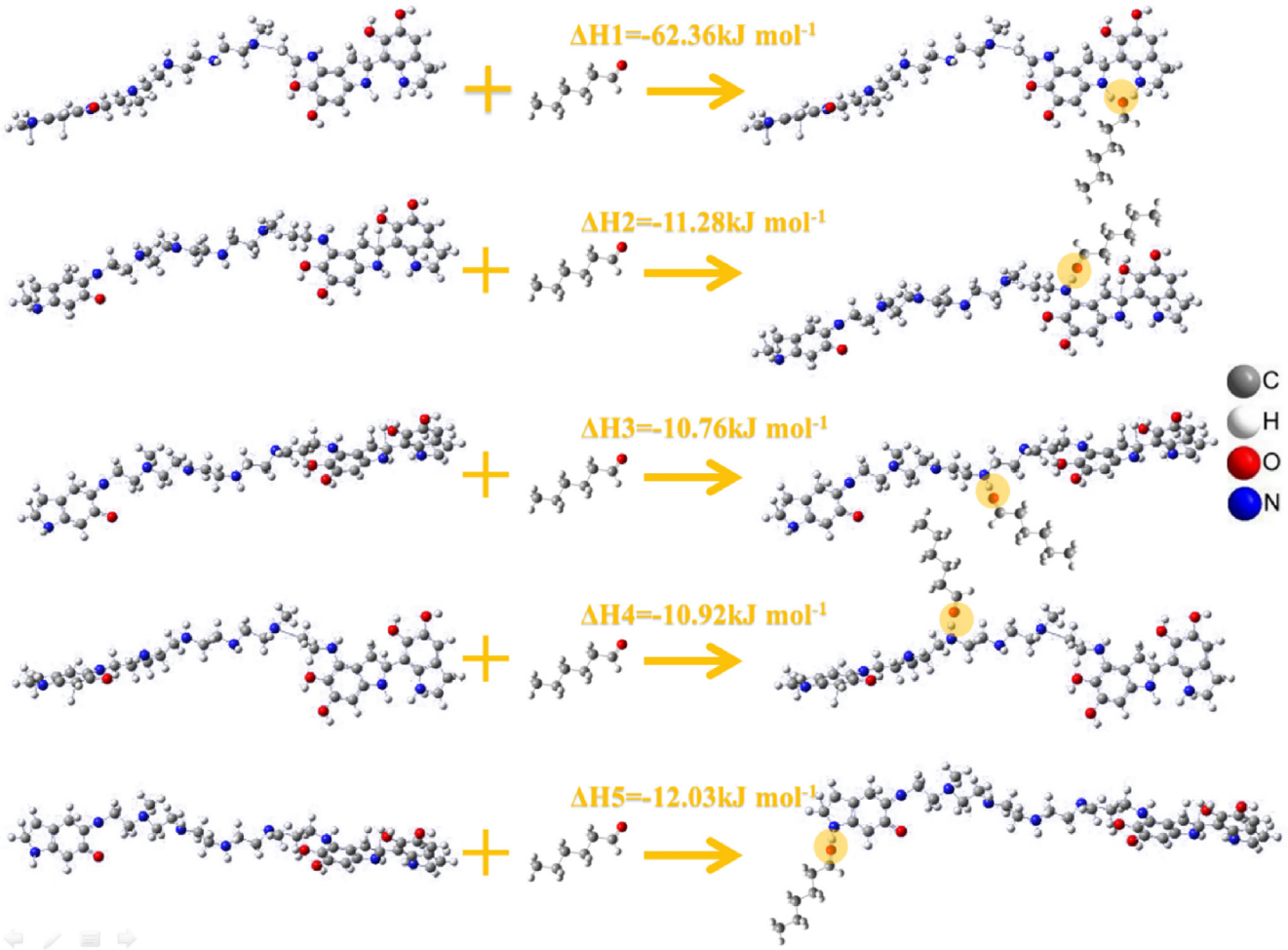

Fig. 9. The Gaussian simulations of hydrogen-bonding adsorption between hexanal molecule and various imino groups of PDA-PEI monomer.

response, response time, recovery time, and sensitivity value. Notably, PODS enhances the lifetime of PDA-PEI-QCM. Superhydrophobic materials work by blocking the formation of intramolecular hydrogen bonds between water molecules. Therefore, in high relative humidity, superhydrophobic PODS layer can block water molecules connected with each other by intramolecular hydrogen bond, and prevent water molecules from coming into contact with PDA. In contrast, there is no intramolecular hydrogen bond between hexanal molecules, and the affinity between hexanal molecule and water molecule is negligible, so hexanal molecules can pass through the PODS layer and contact the PDA layer.

The effect of environmental humidity on the hexanal sensing performance is also investigated in this work. As shown in Fig. 4c, when the environmental humidity increases from 50% to 90% RH, the response change of PODS-PDA-PEI-QCM to hexanal vapor is trivial, indicating the good anti-interference of humidity. It should be attributed to the blocking of water molecule clusters by superhydrophobic PODS, as shown in Fig. 5. Besides, unlike hydrophilic molecules like formaldehyde, hexanal is hardly soluble in water and does not adsorb water molecules. Therefore, water clusters are not pulled by hexanal molecules to enhance the adsorption mass and response in the process of hexanal sensing. Fig. 4d shows the responses of PODS-PDA-PEI-QCM to other three kinds of organic aldehydes (10 ppm) under different humidity environments, including formaldehyde, acetaldehyde and propionaldehyde. In the vacuum environment (~0% RH), the response to hexanal vapor is significantly higher than those of other three aldehydes. It should be attributed to the largest molecular weight of hexanal. However, the increase of environmental humidity causes the response advantage of hexanal vapor to disappear. In high humidity environments, formaldehyde, acetaldehyde and propionaldehyde are mutually soluble in water and therefore have a strong affinity with clusters, so water clusters are introduced during the sensing process. These additional clusters enhance the adsorptive mass and response. Since formaldehyde, acetaldehyde, propionaldehyde, and hexanal all contain aldehyde group, they can be absorbed by the imino group of sensing materialall through weak hydrogen bond adsorption. Therefore, the selectivity difference at low concentrations is not obvious. However, the molecular weight of hexanal is larger than that of the other three organic aldehydes, so when the concentration of gas is increased, the response advantage will be amplified, as shown in Fig. S11.

The dynamic-sensing response of PODS-PDA-PEI-QCM sensor was investigated for detecting trace amount of hexanal vapor. In Fig. 6a, the dynamic-sensing response or frequency change (Hz) versus time is demonstrated, with the hexanal concentration varying from 50 to 250 ppb. All response curves are continuous and stable without obvious basic frequency drift during adsorption and desorption processes. As shown in Fig. S12, the response time distribution of the sensor to low concentration and high concentration hexanal is listed. Obviously, the response time of the sensor to low concentration is longer. It should be attributed to the chemical adsorption between sensing material and hexanal gas with low concentration. On the contrary, too high gas concentration often leads to physical adsorption, because sensing materials can only chemically absorb part of the gas molecules, and most of the remaining gas molecules will physically agglomerate in a short period of time, resulting in rapid response. In Fig. 6b, the sensor responds to 50 ppb hexanal three times in succession. The hexanal

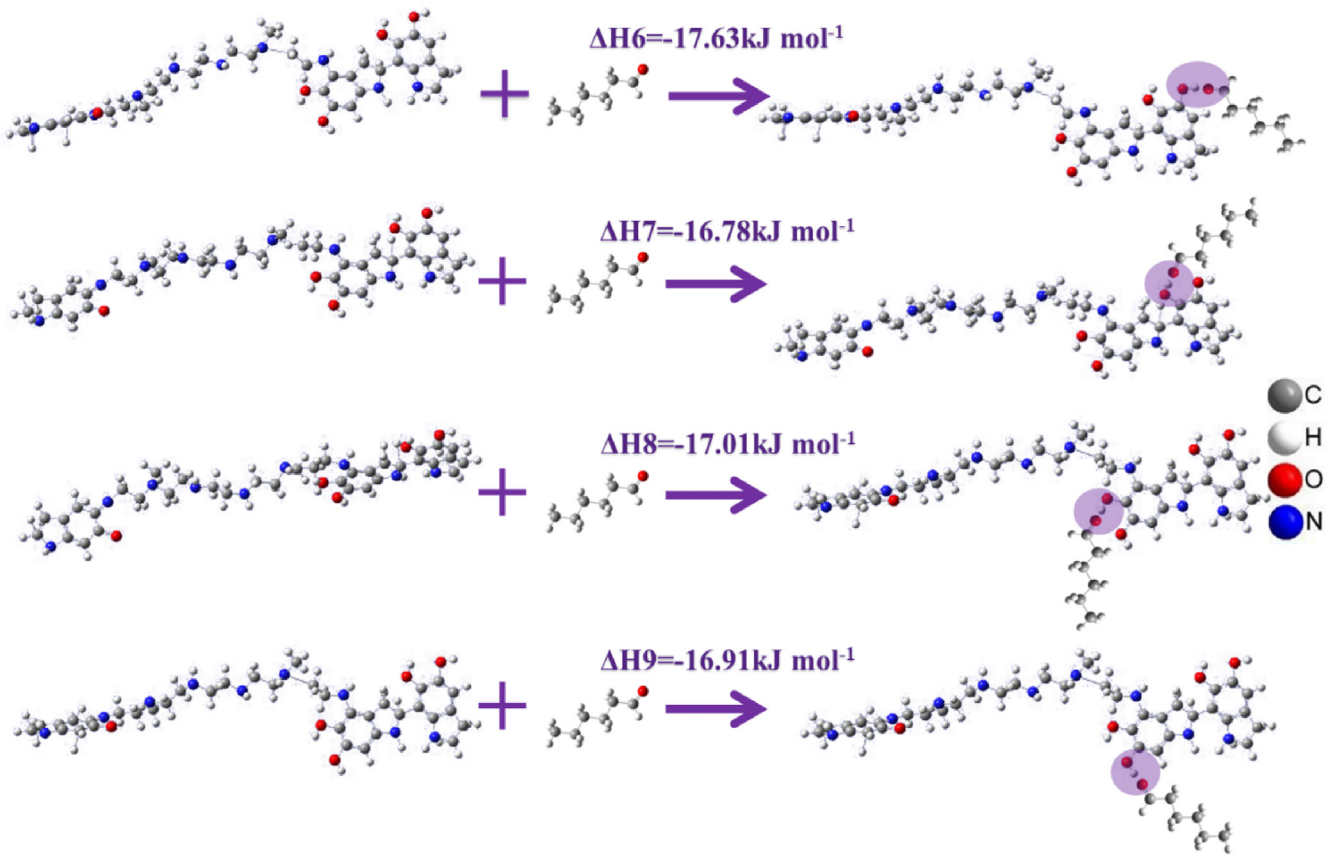

Fig. 10. The Gaussian simulations of hydrogen-bonding adsorption between hexanal molecule and various hydroxyl groups of PDA-PEI monomer.

sensing process exhibits excellent recovery performance, quickly returning to the initial state without response change. This result demonstrates good short-term reproducibility. In addition, as shown in Fig. 6c, the response decrease of PODS-PDA-PEI-QCM to 10 ppm hexanal does not show obvious change for one month in sharp contrast to the rapid decrease of PDA, indicating that the response of PODS-PDA-PEI-QCM to hexanal vapor is also long-term stable. This should be attributed to the self-cleaning ability of superhydrophobic PODS, which is able to withstand environmental pollutants well [44]. As shown in Table 2, the response of PDA-PEI-QCM cannot keep stable within two weeks, while PODS-PDA-PEI-QCM can keep stable in more than one month, indicating a strong contrast in the lifetime of these two sensors. Fig. S13 shows the cyclic response of three different batches of PODS-PDA-PEI-QCM sensors to 50 ppb hexanal. The response values of three batches of sensors in 10 cycles are generally stable, indicating their favorable reproducibility and repeatability. Furthermore, selectivity is considered as another important parameter for gas sensors [45,46]. Fig. 6d exhibited the responses of PODS-PDA-PEI-QCM to several common gases. The response to hexanal vapor is better than other gases with the same concentration, indicating its favorable selectivity for hexanal vapor. In order to further enhance the selectivity of hexanal in the future work, the proportion of PEI in the PDA-PEI copolymer can be increased to introduce amino group (–NH_2). Based on the Schiff base interaction, the (–NH_2) group can detect the gases containing aldehyde group with strong selectivity [5]. Therefore, it has the potential to selectively adsorb the hexanal gas containing aldehyde group.

3.3. Thermodynamic study of the sensor towards hexanal vapor

As a typical mass sensitive device, the response of QCM-based gas sensor depends on the change of the mass, which is caused by the adsorption between gases and sensing materials [47]. The adsorption enthalpy (ΔH) can determine whether the adsorption process is selective and reversible [48]. So far, many reports have revealed that the sensing process is selective and reversible when the ΔH is between −40 and −80 kJ mol^{-1} [49,50]. Fig. 7a and b show the responses of PODS-PDA-PEI-QCM to various concentrations of hexanal vapor at 298 and 313 K. The response of PODS-PDA-PEI-QCM declined with the increase of temperature, revealing the hexanal adsorption exhibits negative Arrhenius temperature dependence. Fig. 7c shows two isotherms, which express the relation between hexanal uptake and hexanal partial pressure at 298 and 313 K. Based on Clausius-Clapeyron equation, ΔH was calculated to be −60.64 kJ mol^{-1}. Therefore, the absorptive sensing process of the sensor to hexanal vapor can be considered as selectivity and reversibility [48].

Exploring the interaction mode between functional group and gas molecule is a way to obtain sensing mechanism. However, there are many different imino groups in PDA-PEI copolymer. It is impractical to use experimental method to explore their roles in the hexanal-sensing process. Therefore, we used simulative calculation to carry out related exploration. Xu and coworkers reported that the covalent crosslinking between PDA and PEI produced a new monomer named PDA-PEI, and the molecular structure is shown in Fig. 8 [39]. The molecular structure is used for the simulation calculation by using Gaussian 09 software. We calculated the ΔH between hexanal and all imino groups in the copolymer monomer by hydrogen bond adsorption. In order to define what situation ΔH1, ΔH2, ΔH3, ΔH4, and ΔH5 represent, we marked the amino groups in different positions (adjacent –NH-1A and –NH-1B, –NH-2, –NH-3, –NH-4, and –NH-5) on the formula of polymer monomer, as shown in Fig. 8. Since the five amino groups at different positions can adsorb hexanal molecules by weak hydrogen bond adsorption, we define the adsorption enthalpy of hexanal at –NH-1A and –NH-1B (two H atoms of adjacent imino groups), –NH-2, –NH-3, –NH-4, and –NH-5 as ΔH1, ΔH2, ΔH3, ΔH4, and ΔH5, respectively. As shown in

Fig. 9, the values of ΔH1, ΔH2, ΔH3, ΔH4, and ΔH5 can be worked out: ΔH1 = −62.36 kJ mol^{-1}, ΔH2 = −11.28 kJ mol^{-1}, ΔH3 = −10.76 kJ mol^{-1}, ΔH4 = −10.92 kJ mol^{-1}, and ΔH5 = −12.03 kJ mol^{-1}. Besides, four hydroxyl groups in the polymer monomer may also adsorb hexanal. We marked the hydroxyl groups in different positions (–OH1, –OH2, –OH3, and –OH4) on the formula of polymer monomer, and we defined the adsorption enthalpy of hexanal at –OH1, –OH2, –OH3, and –OH4 as ΔH6, ΔH7, ΔH8, and ΔH9, respectively. As shown in Fig. 10, the values of ΔH6, ΔH7, ΔH8, and ΔH9 and can be worked out: ΔH6 = −17.63 kJ mol^{-1}, ΔH7 = −16.78 kJ mol^{-1}, ΔH8 = −17.01 kJ mol^{-1}, and ΔH9 = −16.91 kJ mol^{-1}. For ΔH1, two synergistic H-bond adsorptions are formed between the O atom of hexanal and the two H atoms of adjacent imino groups in the copolymer monomer. Its adsorption enthalpy (ΔH1) is −62.36 kJ mol^{-1}, which is smaller than other adsorption enthalpies. The above calculation results indicate that all imino groups and hydroxyl groups of copolymer monomer can play a role in the sensing process, but the two adjacent imino groups are the most important for detecting hexanal.

4. Conclusions

In summary, we reported that a PDA-PEI film containing rich imino groups can induce reversible hydrogen bond adsorption with hexanal molecules, leading to the detecting of ppb-level hexanal vapor. The PODS layer greatly enhances the water-resistance and stability of the PDA-PEI film. The adsorptive sensing mechanism of hexanal vapor has been demonstrated through temperature change experiments and simulation calculations, indicating the important role of the imino sites. Based on QCM, the sensor showed the response of 5.9 Hz and 34.8 Hz to 50 ppb hexanal and 250 ppm hexanal at 25 °C, respectively, and the detection limit of hexanal is even lower to 50 ppb. The strategy in this work may be broadly applicable to other research fields through introducing different functional groups into polymers or copolymers for enhancing stronger adsorptive interactions with gases, thus improving the sensing performance.

Notes

The authors declare no competing financial interest.

Acknowledgements

This work was supported by the Zhejiang Provincial Natural Science Foundation of China (LY20E020001), National Natural Science Foundation of China (51602301 and 51672251), and the Fundamental Research Funds of Zhejiang Sci-Tech University (2019Q007). L. Wang acknowledges Science Foundation of Zhejiang Sci-Tech University, China (ZSTU) under Grant No. 19012393-Y.

Appendix A. Supplementary data

Supplementary data to this article can be found online at https://doi.org/10.1016/j.cej.2020.125755.

References

[1] J.I. Garaycoechea, G.P. Crossan, F. Langevin, L. Mulderrig, S. Louzada, F. Yang, G. Guilbaud, N. Park, S. Roerink, S. Nik-Zainal, M.R. Stratton, K.J. Patel, Alcohol and endogenous aldehydes damage chromosomes and mutate stem cells, Nature 553 (2018) 171.

[2] E. Amini, M.-S. Safdari, J.T. DeYoung, D.R. Weise, T.H. Fletcher, Characterization of pyrolysis products from slow pyrolysis of live and dead vegetation native to the southern United States, Fuel 235 (2019) 1475–1491.

[3] X. Jia, T. Zhang, J. Wang, K. Wang, H. Tan, Y. Hu, L. Zhang, J. Zhu, Responsive photonic hydrogel-based colorimetric sensors for detection of aldehydes in aqueous solution, Langmuir 34 (2018) 3987–3992.

[4] K. Yabushita, A. Yuasa, K. Nagao, H. Ohmiya, Asymmetric catalysis using aromatic aldehydes as chiral α-alkoxyalkyl anions, J. Am. Chem. Soc. 141 (2018) 113–117.

[5] L. Wang, J. Gao, J. Xu, QCM formaldehyde sensing materials: Design and sensing mechanism, Sens. Actuat. B-Chem. 293 (2019) 71–82.

[6] V. Feron, H. Til, F. De Vrijer, R. Woutersen, F. Cassee, P. Van Bladeren, Aldehydes: occurrence, carcinogenic potential, mechanism of action and risk assessment, Mutat. Res.-Gen. Toxicol. Environ. 259 (1991) 363–385.

[7] F. Langevin, G.P. Crossan, I.V. Rosado, M.J. Arends, K.J. Patel, Fancd2 counteracts the toxic effects of naturally produced aldehydes in mice, Nature 475 (2011) 53–58.

[8] Y. Kim, S.-K. Kang, N.-C. Oh, H.-D. Lee, S.-M. Lee, J. Park, H. Kim, Improved sensitivity in schottky contacted two-dimensional MoS2 gas sensor, ACS Appl. Mater. Interfaces 11 (2019) 38902–38909.

[9] G. Bae, I.S. Jeon, M. Jang, W. Song, S. Myung, J. Lim, S.S. Lee, H.-K. Jung, C.-Y. Park, K.-S. An, Complementary dual-channel gas sensor devices based on a role-allocated ZnO/graphene hybrid heterostructure, ACS Appl. Mater. Interfaces 11 (2019) 16830–16837.

[10] E.-X. Chen, H.-R. Fu, R. Lin, Y.-X. Tan, J. Zhang, Highly selective and sensitive trimethylamine gas sensor based on cobalt imidazolate framework material, ACS Appl. Mater. Interfaces 6 (2014) 22871–22875.

[11] H. Yuan, S.A.A.A. Aljneibi, J. Yuan, Y. Wang, H. Liu, J. Fang, C. Tang, X. Yan, H. Cai, Y. Gu, S.J. Pennycook, J. Tao, D. Zhao, ZnO nanosheets abundant in oxygen vacancies derived from metal-organic frameworks for ppb-level gas sensing, Adv. Mater. 31 (2019).

[12] O. Moncea, J. Casanova-Chafer, D. Poinsot, L. Ochmann, C.D. Mboyi, H.O. Nasrallah, E. Llobet, I. Makni, M. El Atrous, S. Brandes, Y. Rousselin, B. Domenichini, N. Nuns, A.A. Fokin, P.R. Schreiner, J.-C. Hierso, Diamondoid nanostructures as sp(3)- carbon- based gas sensors, Angew. Chem. Int. Ed. 58 (2019) 9933–9938.

[13] M. Zhang, X.X. Wang, W.Q. Cao, J. Yuan, M.S. Cao, Electromagnetic functions of patterned 2D materials for micro–nano devices covering GHz, THz, and optical frequency, Adv. Opt. Mater. 7 (2019) 1900689.

[14] M.S. Cao, X.X. Wang, M. Zhang, J.C. Shu, W.Q. Cao, H.J. Yang, X.Y. Fang, J. Yuan, Electromagnetic response and energy conversion for functions and devices in low-dimensional materials, Adv. Funct. Mater. 29 (2019) 1807398.

[15] Z. Ma, T. Yuan, Y. Fan, L. Wang, Z. Duan, W. Du, D. Zhang, J. Xu, A benzene vapor sensor based on a metal-organic framework-modified quartz crystal microbalance, Sens. Actuat. B-Chem. 311 (2020) 1900689.

[16] N. Liu, Y. Fan, Z. Ma, H. Lin, J. Xu, Materials design and sensing mechanism of novel calix[6]arene composite for sensitively detecting amine drugs, Chin. Chem. Lett. doi: 10.1016/j.cclet.2020.01.034.

[17] D. Wang, L. Tian, H. Li, K. Wan, X. Yu, P. Wang, A. Chen, X. Wang, J. Yang, Mesoporous ultrathin SnO2 nanosheets in situ modified by graphene oxide for extraordinary formaldehyde detection at low temperatures, ACS Appl. Mater. Interfaces 11 (2019) 12808–12818.

[18] K. Iitani, P.-J. Chien, T. Suzuki, K. Toma, T. Arakawa, Y. Iwasaki, K. Mitsubayashi, Fiber-optic bio-sniffer (biochemical gas sensor) using reverse reaction of alcohol dehydrogenase for exhaled acetaldehyde, ACS Sens. 3 (2018) 425–431.

[19] L. Ernstgård, A. Iregren, B. Sjögren, U. Svedberg, G. Johanson, Acute effects of exposure to hexanal vapors in humans, J Occup. Environ. Med. 48 (2006) 573–580.

[20] S. Janfaza, M.B. Nojavani, M. Nikkhah, T. Alizadeh, A. Esfandiar, M.R. Ganjali, A selective chemiresistive sensor for the cancer-related volatile organic compound hexanal by using molecularly imprinted polymers and multiwalled carbon nanotubes, Microchim. Acta 186 (2019) 137.

[21] P. Fuchs, C. Loeseken, J.K. Schubert, W. Miekisch, Breath gas aldehydes as biomarkers of lung cancer, Int. J. Cancer 126 (2010) 2663–2670.

[22] V.V. Quang, V.N. Hung, L.A. Tuan, V.N. Phan, T.Q. Huy, N.V. Quy, Graphene-coated quartz crystal microbalance for detection of volatile organic compounds at room temperature, Thin Solid Films 568 (2014) 6–12.

[23] B. Wyszynski, P. Somboon, T. Nakamoto, Pegylated lipids as coatings for QCM odor-sensors, Sens. Actuat. B-Chem. 121 (2007) 538–544.

[24] W. Chen, Z. Wang, S. Gu, J. Wang, Detection of hexanal in humid circumstances using hydrophobic molecularly imprinted polymers composite, Sens. Actuat. B-Chem. 291 (2019) 141–147.

[25] M.E. Escuderos, S. Sanchez, A. Jimenez, Application of a quartz crystal microbalance (QCM) system coated with chromatographic adsorbents for the detection of olive oil volatile compounds, J. Sens. Technol. 1 (2011) 1–8.

[26] S.K. Jha, K. Hayashi, A quick responding quartz crystal microbalance sensor array based on molecular imprinted polyacrylic acids coating for selective identification of aldehydes in body odor, Talanta 134 (2015) 105–119.

[27] W. Chen, Z. Wang, S. Gu, J. Wang, Y. Wang, Z. Wei, Detection of hexanal and 1-octen-3-ol in refrigerated grass carp fillets using a QCM gas sensor based on hydrophobic Cu(I)-Cys nanocomposite, Sens. Actuat. B-Chem. 305 (2020) 127476.

[28] J. Lin, N. Gao, J. Liu, Z. Hu, H. Fang, X. Tan, H. Li, H. Jiang, H. Liu, T. Shi, G. Liao, Superhydrophilic $Cu(OH)_2$ nanowire- based QCM transducer with self- healing ability for humidity detection, J. Mater. Chem. A 7 (2019) 9068–9077.

[29] D.-J. Li, Z.-G. Gu, I. Vohra, Y. Kang, Y.-S. Zhu, J. Zhang, Epitaxial growth of oriented metalloporphyrin network thin film for improved selectivity of volatile organic compounds, Small 13 (2017).

[30] S. Wannapaiboon, A. Schneemann, I. Hante, M. Tu, K. Epp, A.L. Semrau, C. Sternemann, M. Paulus, S.J. Baxter, G. Kieslich, R.A. Fischer, Control of structural flexibility of layered-pillared metal-organic frameworks anchored at surfaces, Nat. Commun. 10 (2019).

[31] L. Wang, Y. Zhu, Q. Xiang, Z. Cheng, Y. Chen, J. Xu, One novel humidity-resistance formaldehyde molecular probe based hydrophobic diphenyl sulfone urea dry-gel: synthesis, sensing performance and mechanism, Sens. Actuat. B-Chem. 251 (2017) 590–600.

[32] L. Michalek, K. Mundsinger, C. Barner-Kowollik, L. Barner, The long and the short of polymer grafting, Polym. Chem.-UK 10 (2019) 54–59.

[33] C. Liu, L. Shang, H.-T. Yoshioka, B. Chen, K. Hayashi, Preparation of molecularly imprinted polymer nanobeads for selective sensing of carboxylic acid vapors, Anal.

Chim. Acta 1010 (2018) 1–10.
[34] S.J. Higgins, Conjugated polymers incorporating pendant functional groups—synthesis and characterisation, Chem. Soc. Rev. 26 (1997) 247–257.
[35] A. Mirmohseni, V. Hassanzadeh, Application of polymer-coated quartz crystal microbalance (QCM) as a sensor for BTEX compounds vapors, J. Appl. Polym. Sci. 79 (2001) 1062–1066.
[36] N. Wang, X. Wang, Y. Jia, X. Li, J. Yu, B. Ding, Electrospun nanofibrous chitosan membranes modified with polyethyleneimine for formaldehyde detection, Carbohydr. Polym. 108 (2014) 192–199.
[37] S. Lo Schiavo, P. Cardiano, N. Donato, M. Latino, G. Neri, A dirhodium(II, II) complex as a highly selective molecular material for ammonia detection: QCM studies, J. Mater. Chem. 21 (2011) 18034–18041.
[38] D. Yan, P. Xu, Q. Xiang, H. Mou, J. Xu, W. Wen, X. Li, Y. Zhang, Polydopamine nanotubes: bio-inspired synthesis, formaldehyde sensing properties and thermodynamic investigation, J. Mater. Chem. A 4 (2016) 3487–3493.
[39] H.-C. Yang, K.-J. Liao, H. Huang, Q.-Y. Wu, L.-S. Wan, Z.-K. Xu, Mussel-inspired modification of a polymer membrane for ultra-high water permeability and oil-in-water emulsion separation, J. Mater. Chem. A 2 (2014) 10225–10230.
[40] L. Wang, Y. Yu, Q. Xiang, J. Xu, Z. Cheng, J. Xu, PODS-covered PDA film based formaldehyde sensor for avoiding humidity false response, Sens. Actuat. B-Chem. 255 (2018) 2704–2712.
[41] Q. Ke, G. Li, Y. Liu, T. He, X.-M. Li, Formation of superhydrophobic polymerized n-octadecylsiloxane nanosheets, Langmuir 26 (2010) 3579–3584.
[42] Y. Tian, Y. Cao, Y. Wang, W. Yang, J. Feng, Realizing ultrahigh modulus and high strength of macroscopic graphene oxide papers through crosslinking of mussel-inspired polymers, Adv. Mater. 25 (2013) 2980–2983.
[43] J.H. Lee, S. Kim, T.Y. Kim, U. Khan, S.-W. Kim, Water droplet-driven triboelectric nanogenerator with superhydrophobic surfaces, Nano Energy 58 (2019) 579–584.
[44] Y. Lu, S. Sathasivam, J. Song, C.R. Crick, C.J. Carmalt, I.P. Parkin, Robust self-cleaning surfaces that function when exposed to either air or oil, Science 347 (2015) 1132–1135.
[45] X. Wu, S. Xiong, Z. Mao, S. Hu, X. Long, A designed ZnO@ZIF-8 core-shell nanorod film as a gas sensor with excellent selectivity for H-2 over CO, Chem-Eur. J. 23 (2017) 7969–7975.
[46] Z. Wang, A. Sackmann, S. Gao, U. Weimar, G. Lu, S. Liu, T. Zhang, N. Barsan, Study on highly selective sensing behavior of ppb-level oxidizing gas sensors based on Zn2SnO4 nanoparticles immobilized on reduced graphene oxide under humidity conditions, Sens. Actuat. B-Chem. 285 (2019) 590–600.
[47] D. Zhang, Y. Fan, G. Li, W. Du, R. Li, Y. Liu, Z. Cheng, J. Xu, Biomimetic synthesis of zeolitic imidazolate frameworks and their application in high performance acetone gas sensors, Sens. Actuat. B-Chem. 302 (2020) 127187.
[48] P. Xu, H. Yu, S. Guo, X. Li, Microgravimetric thermodynamic modeling for optimization of chemical sensing nanomaterials, Anal. Chem. 86 (2014) 4178–4187.
[49] J. Zong, Y.S. Zhang, Y. Zhu, Y. Zhao, W. Zhang, Y. Zhu, Rapid and highly selective detection of formaldehyde in food using quartz crystal microbalance sensors based on biomimetic poly-dopamine functionalized hollow mesoporous silica spheres, Sens. Actuat. B-Chem. 271 (2018) 311–320.
[50] P. Xu, H. Yu, X. Li, Microgravimetric analysis method for activation-energy extraction from trace-amount molecule adsorption, Anal. Chem. 88 (2016) 4903–4908.